LEVEL II

12 mc

SDAC-TR-79-9

RELATIONSHIP BETWEEN M_s AND m_b FOR SMALL EARTHQUAKES IN UZBEKISTAN, USSR

J.H. Gonez & I.T. Noponen
Seismic Data Analysis Center
Teledyne Geotech, 314 Montgomery Street, Alexandria Virginia 22314

13 December 1979

APPROVED FOR PUBLIC RELEASE; DISTRIBUTION UNLIMITED.

Sponsored by
The Defense Advanced Research Projects Agency (DARPA)
DARPA Order No. 2551

Monitored By
AFTAC/VSC
312 Montgomery Street, Alexandria, Virginia 22314

Disclaimer: Neither the Defense Advanced Research Projects Agency nor the Air Force Technical Applications Center will be responsible for information contained herein which has been supplied by other organizations or contractors, and this document is subject to later revision as may be necessary. The views and conclusions presented are those of the authors and should not be interpreted as necessarily representing the official policies, either expressed or implied, of the Defense Advanced Research Projects Agency, the Air Force Technical Applications Center, or the US Government.

Unclassified

SECURITY CLASSIFICATION OF THIS PAGE (When Data Entered)

REPORT DOCUMENTATION PAGE

READ INSTRUCTIONS BEFORE COMPLETING FORM

1. REPORT NUMBER: SDAC-TR-79-9
2. GOVT ACCESSION NO.: AD-A091 984
3. RECIPIENT'S CATALOG NUMBER:

4. TITLE (and Subtitle): RELATIONSHIP BETWEEN M_s AND m_b FOR SMALL EARTHQUAKES IN UZBEKISTAN, USSR
5. TYPE OF REPORT & PERIOD COVERED: Technical rept.
6. PERFORMING ORG. REPORT NUMBER:

7. AUTHOR(s): John Goncz, Ilkka Noponen
8. CONTRACT OR GRANT NUMBER(s): F08606-79-C-0007, DARPA Order-2551

9. PERFORMING ORGANIZATION NAME AND ADDRESS
Teledyne Geotech
314 Montgomery Street
Alexandria, Virginia 22314

10. PROGRAM ELEMENT, PROJECT, TASK AREA & WORK UNIT NUMBERS: VT/9709 12 41

11. CONTROLLING OFFICE NAME AND ADDRESS
Defense Advanced Research Projects Agency
Nuclear Monitoring Research Office
1400 Wilson Blvd., Arlington, Virginia 22209

12. REPORT DATE: 13 December 1979
13. NUMBER OF PAGES: 37

14. MONITORING AGENCY NAME & ADDRESS (if different from Controlling Office)
VELA Seismological Center
312 Montgomery Street
Alexandria, Virginia 22314

15. SECURITY CLASS. (of this report): Unclassified
15a. DECLASSIFICATION/DOWNGRADING SCHEDULE:

16. DISTRIBUTION STATEMENT (of this Report)

APPROVED FOR PUBLIC RELEASE; DISTRIBUTION UNLIMITED.

17. DISTRIBUTION STATEMENT (of the abstract entered in Block 20, if different from Report)

18. SUPPLEMENTARY NOTES

19. KEY WORDS (Continue on reverse side if necessary and identify by block number)
M_s:m_b
Discrimination
Body Wave Magnitude
Wave Absorption
delta M_s / delta m_b

20. ABSTRACT (Continue on reverse side if necessary and identify by block number)

The SRO station MAIO was used to obtain many measurements of P_n and LR from a sequence of aftershocks at Gazli, Uzbekistan in 1976, at a distance of 576 km. SP periods and amplitudes are analyzed to obtain the proper distance correction factor to yield m_b. Eighteen events are measured to give an M_s range 2.2 to 3.6, and m_b range 3.6 to 5.0. The observations support the postulation that $\partial M_s / \partial m_b \approx 1$ at low magnitudes. The Gazli population overlaps a Eurasian teleseismic population, and is believed to be free of

is approximately equal to

DD FORM 1 JAN 73 1473 EDITION OF 1 NOV 65 IS OBSOLETE

Unclassified

SECURITY CLASSIFICATION OF THIS PAGE (When Data Entered)

JOB

4108258

large error in determination of M_s and m_b.

RELATIONSHIP BETWEEN M_s AND m_b FOR SMALL EARTHQUAKES IN UZBEKISTAN, USSR

SEISMIC DATA ANALYSIS CENTER REPORT NO.: SDAC-TR-79-9

AFTAC Project Authorization No.:	VELA T/9707/B/ETR
Project Title:	Seismic Data Analysis Center
ARPA	2551
Name of Contractor:	TELEDYNE GEOTECH
Contract No.:	F08606-79-C-0007
Date of Contract	01 October 1979
Amount of Contract:	$279,929
Contract Expiration Data:	30 September 1980
Project Manager	Robert R. Blandford (703) 836-3882

P.O. Box 334, Alexandria, Virginia 22313

APPROVED FOR PUBLIC RELEASE; DISTRIBUTION UNLIMITED.

ABSTRACT

The SRO station MAIO was used to obtain many measurements of P_n and LR from a sequence of aftershocks at Gazli, Uzbekistan in 1976, at a distance of 576 km. SP periods and amplitudes are analyzed to obtain the proper distance correction factor to yield m_b. Eighteen events are measured to give an M_s range 2.2 to 3.6, and m_b range 3.6 to 5.0. The observations support the postulation that $\partial M_s/\partial m_b \approx 1$ at low magnitudes. The Gazli population overlaps a Eurasian teleseismic population, and is believed to be free of large error in determination of M_s and m_b.

TABLE OF CONTENTS

	Page
ABSTRACT	2
LIST OF FIGURES	4
LIST OF TABLES	6
INTRODUCTION	7
DATA PROCESSING	9
MEASUREMENT OF M_s MAGNITUDES	15
MEASUREMENT OF m_b MAGNTIUDES	19
Summary	19
Additional Comments	26
SIMULATED m_b VERSUS M_s RELATIONSHIP	27
OBSERVATIONS OF L_g AND P_n AMPLITUDES	29
SATURATION AT SRO STATIONS	30
RESULTS AND CONCLUSIONS	32
ACKNOWLEDGEMENTS	35
REFERENCES	36

LIST OF FIGURES

Figure No		Page
1	Location of the earthquake aftershock sequence at Gazli, and the SRO station MAIO. The asterisks show the geographical distribution of earthquakes and the symbol □ denotes explosions recorded at NORSAR (Bungum and Tjostheim, 1976) used for comparison with the Gazli sequence.	10
2	Gazli aftershock sequence recorded at MAIO, short-period channel. These are continuous recordings and each trace is 3 minutes 16 seconds long. Event 1 of this report is on the top trace.	11
3	Gazli aftershock sequence recorded at MAIO, three-component long-period. Event 1 on uppermost trace. Middle set of traces shows non-linear response apparently due to large short-period signal (see corresponding short-period signal in Figure 2).	13
4	Event number 17 surface waves recorded at NUR, M_S = 4.2 (above) and KBL, M_S = 3.5 (below). These are WWSSN stations and the timing marks are at one-minute intervals.	17
5	Station bias of 0.3 M_S units is evident when regional M_S values are plotted against WWSSN teleseismic values.	18
6	Periods of P_n, Gazli aftershock sequence, plotted against peak-to-peak observed amplitude of P_n. For small shocks the period is constant and equal to about 0.4 sec. As the shock strength increases, the period of P_n gets longer. Thick line gives the simulated period vs. amplitude relationship.	20
7	Theoretical response of P-wave signals after modification by attenuation and SRO instrument response.	22
8	Difference in m_b plotted against Mashad trace amplitude for simulated seismograms using different formulas for Mashad m_b.	23
9	The correlation between attenuation-corrected log A/T values and teleseismic values of m_b.	25
10	Simulated relation between $\log_{10} I$ (I, the P-wave pulse area, is proportional to seismic moment), and m_b.	28
11	P_n and L_g recorded at MAIO from Gazli earthquake aftershock sequence 8 April 1976.	29

LIST OF FIGURES (Continued)

Figure No.	Title	Page
12	Progressively greater shocks from top trace to bottom, showing development of non-linear recording on the long-period channel. The traces are different sweep speeds, of course, but they are aligned at the instant of time corresponding to the S_n phase.	31
13	Gazli aftershock sequence (open circles) of events plotted together with Eurasian earthquakes (filled circles) recorded at NORSAR. The straight lines shown are *maximum*-likelihood slopes assuming equal distributions of error in both M_s and m_b for the two populations separately. The two populations though shown together here, should not be combined into one population because of possible small systematic differences in magnitude determinations.	33

LIST OF TABLES

Table No.	Title	Page
I	Earthquakes in the Gazli aftershock sequence used in this study.	14

INTRODUCTION

This report describes the acquisition and processing of seismic waveforms from the aftershock sequence of the Gazli earthquake of 02 hours 40 minutes 23.9 seconds on April 8, 1976. This project was started with three objectives in view:

- Extend M_s:m_b measurements to low values;
- Provide experimental observations to test the theoretical concept that $\frac{\partial M_s}{\partial m_b} = 1$ at small values of magnitude; and
- Investigate the difficulties in using regional measurements of magnitude in conjunction with teleseismic measurements of magnitude.

In order to make magnitude measurements of low energy earthquakes, the receiving seismograph must be located close to the epicenter; otherwise the surface waves will be attenuated so much that they will be lost in the earth noise at the receiver.

In the present experiment the Seismic Research Observatory (SRO) station Mashad, Iran (station designator MAIO), located 576 km from the epicenter of the major shock, was used as the only receiving seismograph because it was the only digital system in operation at the time. The SRO digital seismic system has a dynamic recording range of 60 dB for short-period and 120 dB for long-period. It was hoped to exploit this wide dynamic range to gather a range of magnitude values from the largest value 6.2 m_b of the main shock, down to the earth noise level equivalent to 3.0 m_b at the Gazli distance. This potential magnitude range of 3.2 magnitude units, equivalent to 63 dB, is considerably greater than the 40 dB dynamic range recording capability of a WWSSN station, and would give the opportunity to tie in these lower M_s:m_b measurements with the more abundant larger values existing in the literature.

It was found that the upper range of m_b values was limited by nonlinear effects in the analog part of the SRO system which became apparent at 5.2 m_b, thus precluding the possibility of larger m_b measurements with the same source-station combination. Apparently the large amplitude high frequency signal associated with the phase S_n saturates the early stages of

amplification and causes the long-period signal to lose fidelity. The long time constant of the filters in the LP sections cause LP distortion to persist for several minutes although it appears that the SP signal regains its fidelity within several seconds.

In this report the acquisition procedures are described, followed by a discussion of the formulas and procedures used to calculate M_s and m_b. An interpretation of the systematic increase of P_n period with amplitude is used to estimate the attenuation of the path, and by using this estimate, to obtain the distance correction factor for this geographical path.

Our M_s:m_b results are presented in the context of Eurasian earthquakes determined at teleseismic distance by Bungum and Tjostheim (1976) with the NORSAR array. The two populations, observed with two very different instruments, appear to form a coherent pattern.

Bungum, H. and D. Tjostheim (1976). Discrimination between Eurasian earthquakes and underground explosions using the m_b:M_s method and short-period autoregressive parameters, Geophys. J. R. Astr. Soc., 45, 371-392.

DATA PROCESSING

The main shock which caused extensive damage in the town of Gazli in Uzbekistan, USSR, occurred on April 8, 1976 at 02 hours 40 minutes 23.9 seconds, 40.31°N latitude and 63.72°E longitude and had an m_b = 6.2 according to the ISC bulletin. Figure 1 shows the location of Gazli and MAIO. The extended aftershock sequence which developed continued for a period of three months before the reported rate of earthquakes fell below two per month. Although the SRO system is detection-triggered for SP recordings, the high rate of activity during the first 24 hours provided almost continuous recording, which facilitated searching for small events that might not have triggered the recording system.

Plots of the quasi-continuous SP recording were produced from the digital tapes and searched for signal arrivals. Figure 2 shows the plot format and an example of the excellent signal quality produced by the SRO system.

Jeffreys-Bullen seismological tables established that the earliest arrival was P_n and the following characteristic impulsive high frequency phase was S_n. The following extended lower frequency phase is L_g with a maximum amplitude propagating at a group velocity of about 3.1 km/sec. The usual velocity for L_g is 3.5 km/sec, but there is no phase visible at this velocity in these recordings because of the emergent nature of L_g along this path.

The short, impulsive phase S_n was useful in detecting the smaller events where it was very difficult to find P_n by itself. S_n was easy to recognize and the constant time differential of 61 sec between P_n and S_n established the location of P_n. Once an origin time was established, the separately plotted long-period three-component signal was examined for surface waves visible above the background noise. The velocities of the various phases examined in this report, based on a 570 km long path were:

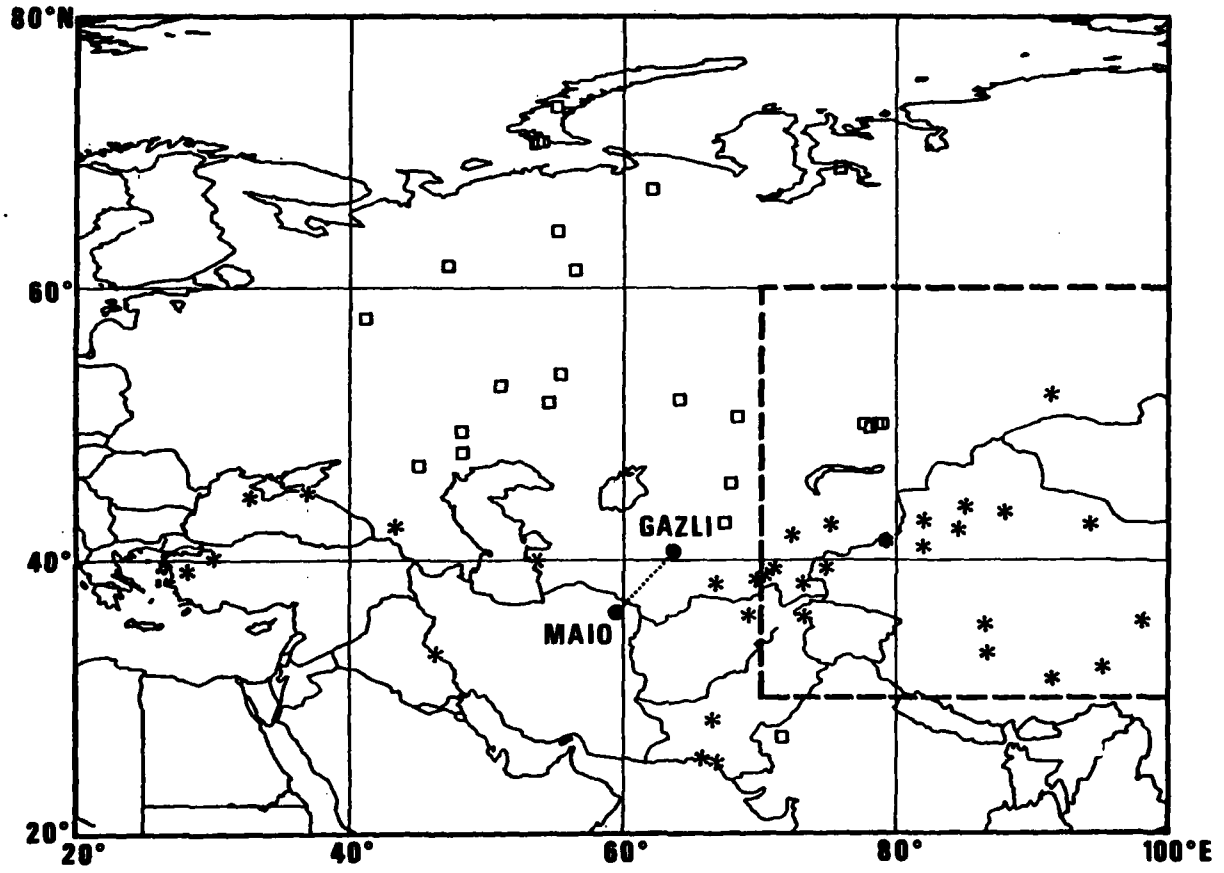

Figure 1. Location of the earthquake aftershock sequence at Gazli, and the SRO station MAIO. The asterisks show the geographical distribution of earthquakes and the symbol □ denotes explosions recorded at NORSAR (Bungum and Tjostheim, 1976) used for comparison with the Gazli sequence.

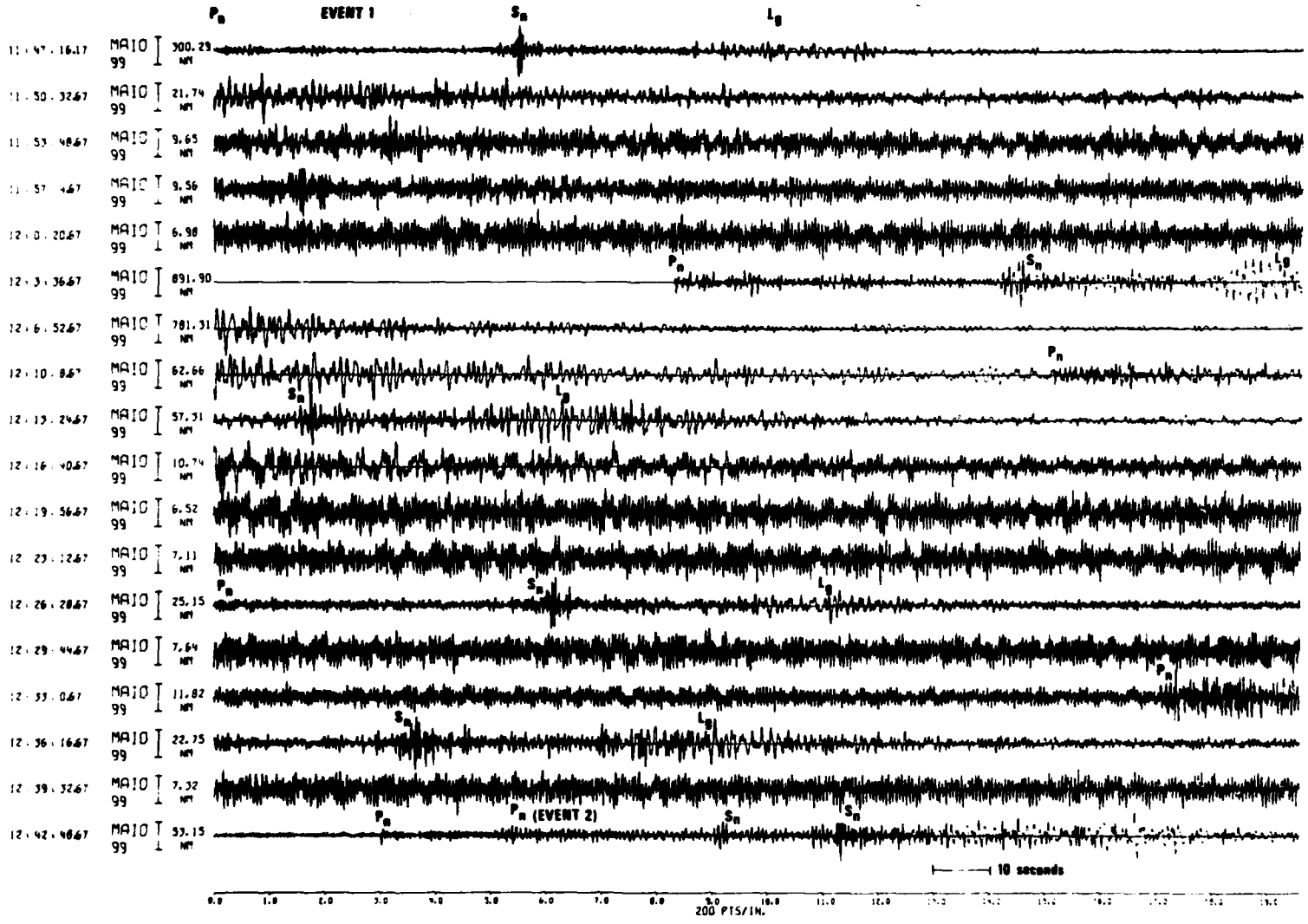

Figure 2. Gazli aftershock sequence recorded at MAIO, short-period channel. These are continuous recordings and each trace is 3 minutes 16 seconds long. Event 1 of this report is on the top trace.

Phase	Velocity km/sec	Travel Time seconds
P_n	7.38	78
S_n	4.16	138.5
L_g (maximum)	3.06	188
Surface Wave-Long Period	2.94	196

The surface waves in all events were well developed dispersed waves with apparent periods from 18 to 25 seconds with the peak amplitude occurring generally at 20 seconds as shown in Figure 3. The surface waves were visible on all three components with comparable amplitudes. The threshold for detection of surface waves determined by minimum earth noise of about 25 nanometers peak-to-peak, which corresponds to an M_s of 2.2 at Gazli.

The earthquakes selected for use in this study are listed in Table I. The first twenty-four hours of the aftershock sequence were used to find small magnitude events because the short-period detector was triggered almost continously during that time. Later, the NEIS bulletin was used to identify some larger events so that the full dynamic range capability of MAIO could be used.

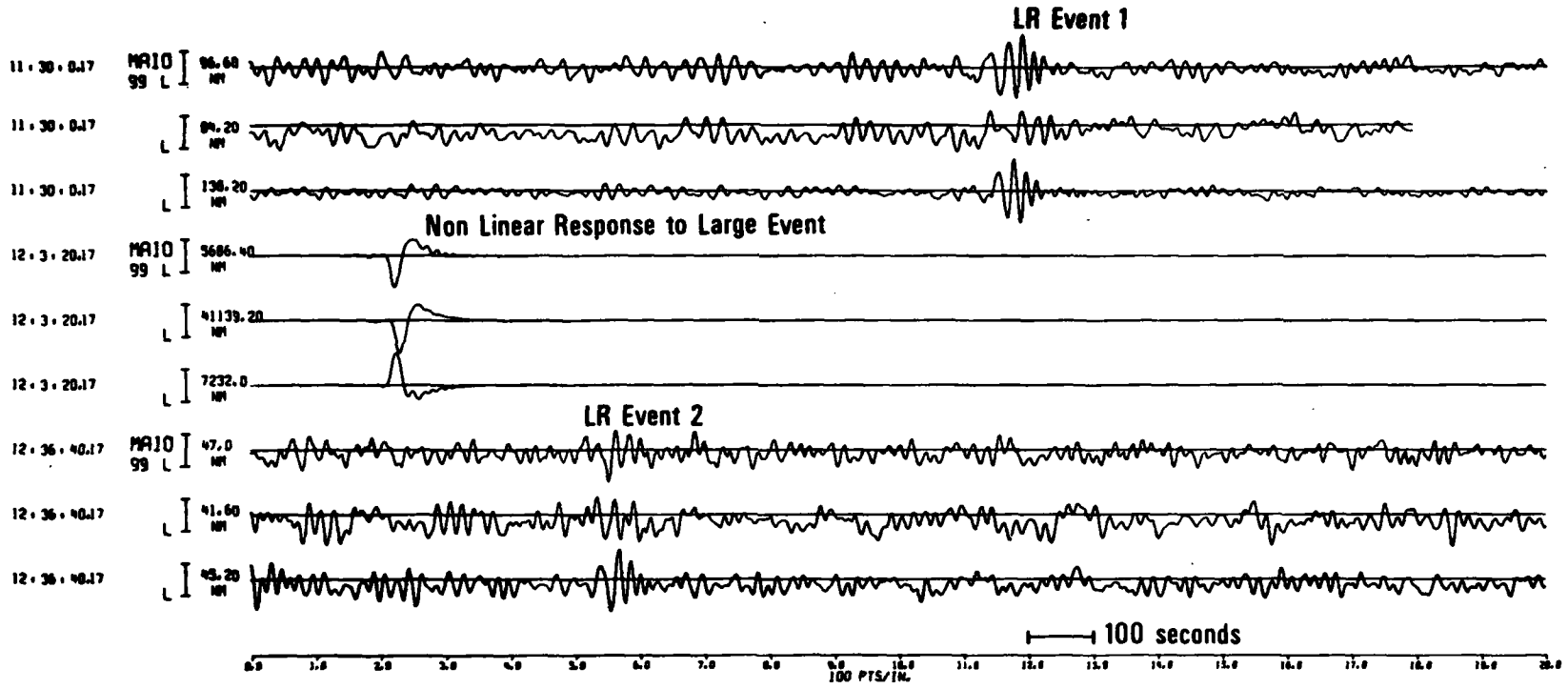

Figure 3. Gazli aftershock sequence recorded at MAIO, three-component long-period. Event 1 on uppermost trace. Middle set of traces shows non-linear response apparently due to large short-period signal (see corresponding short-period signal in Figure 2).

TABLE I

Earthquakes in the Gazli Aftershock Sequence
Used in This Study

Event Number	Date	Origin Time	m_b	M_s
1	08 Apr 76	11:45:49.7	4.2	3.1
2	08 Apr 76	12:42:06.7	3.6	2.7
3	08 Apr 76	14:27:09.3	3.9	2.5
4	08 Apr 76	14:41:28.0	3.8	2.6
5	08 Apr 76	15:26:52.7	3.9	2.7
6	08 Apr 76	17:03:33.2	3.9	2.5
7	08 Apr 76	18:39:38.2	3.7	2.6
8	08 Apr 76	22:54:17.7	4.3	3.1
9	09 Apr 76	01:09:26.8	3.6	2.7
10	09 Apr 76	02:46:24.9	4.5	3.0
11	09 Apr 76	03:59:19.3	3.7	2.2
12	23 Apr 76	01:56:48.3	5.0	3.9
13	23 Apr 76	20:55:31.7	4.6	3.7
14	05 May 76	12:49:14.8	4.2	3.1
15	07 May 76	00:10:48.4	4.9	3.6
16	17 May 76	11:01:26.3	4.2	3.2
17	17 May 76	17:46:17.2	4.6	3.6
18	19 May 76	01:11:20.8	4.4	2.8

MEASUREMENT OF M_s MAGNITUDES

We decided to use the M_s formula suggested by von Seggern (1977), which is written as

$$M_s = \log(\text{amplitude}) + 1.08 \log\Delta - 0.22$$

rather than those given by Vanek et al. (1962), Evernden (1971) or Marshall and Basham (1972), since von Seggern's re-estimation of the amplitude variation as the function of distance is based on the modern WWSSN LP network and a very large number of amplitude readings. The results by von Seggern deviate significantly from those implied by the "Prague" magnitude formula

$$M_s = \log\left(\frac{A}{T}\right) + 1.66 \log\Delta - 0.18$$

and the latter is thus in doubt. Also, the amplitude variation observed by von Seggern is predictable from wave propagation theory after fitting a single parameter, the wave absorption, to the observations. Thus its extension to distances as short as 5°, far shorter than von Seggern's observations, has a sound base.

Because the possibility of creating a station bias would be high if we were to use only the M_s values determined at MAIO as described, we sought to establish if such a bias were present by using all available WWSSN station

von Seggern, David (1977). Amplitude-distance relation for 20-second Rayleigh waves, Bull. Seism. Soc. Am., 67, 405-411.

Vanek, J., A. Zatopek, V. Karnik, N. V. Konderskaya, Y. V. Rizmichenko, E. F. Savarensky, S. L. Solovev, N. V. Shebalin (1962). Standardization of magnitude scales, Bull. (Izvest.) Acad. Sci. U.S.S.R., Geophys. Ser., 2, 108.

Evernden, J. F. (1971). Variation of Rayleigh-wave amplitude with distance, Bull. Seism. Soc. Am., 61, 231.

Marshall, P. D. and D. W. Basham (1972). Discrimination between earthquakes and underground explosions employing an improved M_s scale, Geophys. J. R. Astr. Soc., 28, 431-458.

records of the larger events. The larger events were recorded at distances as great as 36.6° (COP-Copenhagen, Denmark) and 31.3° (NUR-Nurmijärvi, Finland). Figure 4 shows the Rayleigh waves for event 17, M_s = 3.6, at NUR where its amplitude is just above threshold, and the same event also at Kabul, Afghanistan (Δ = 7.1°) where the amplitude is much higher. In addition to the 20-second dispersed wavetrain, note the 4 to 6 second dispersed wavetrain which was not seen in the MAIO waveforms due, presumably due to the difference in instrument responses.

There were 43 measurements of M_s-WWSSN available for 7 of the Gazli aftershock earthquakes. This information is plotted in Figure 5 and establishes an MAIO station bias of -0.3 magnitude units.

Thus, for the final M_s value used in this study, 0.3 was added to each M_s measurement determined by von Seggern's formula.

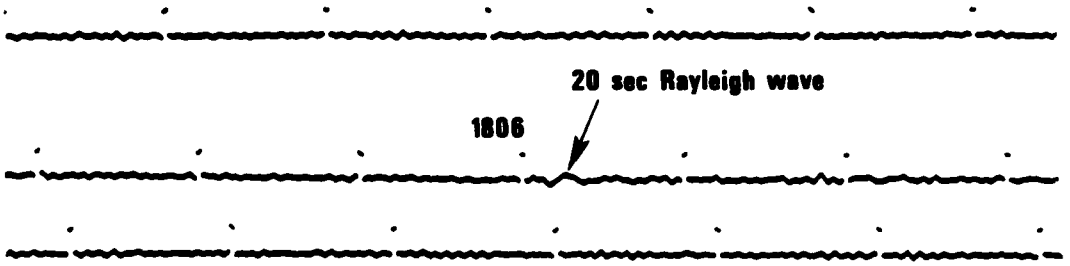

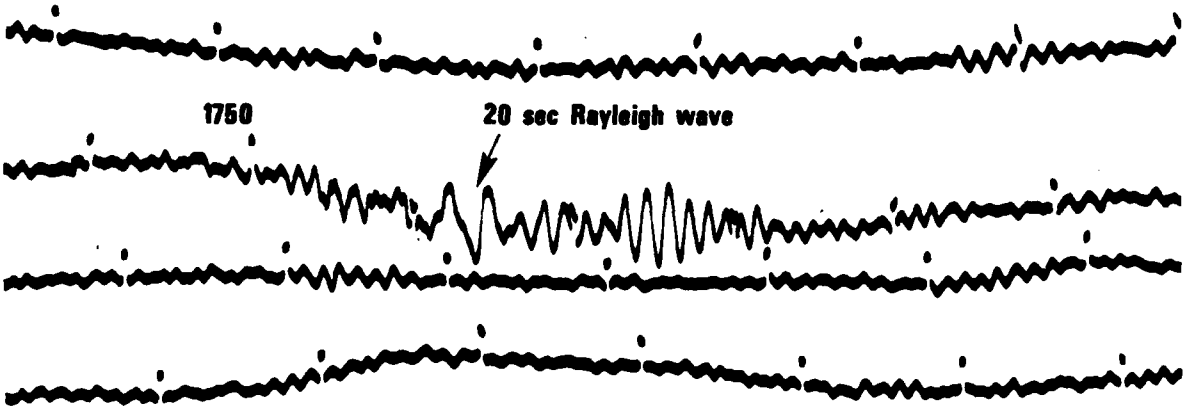

Figure 4. Event number 17 surface waves recorded at NUR, M_s = 4.2 (above) and KBL, M_s = 3.5 (below). These are WWSSN stations and the timing marks are at one-minute intervals.

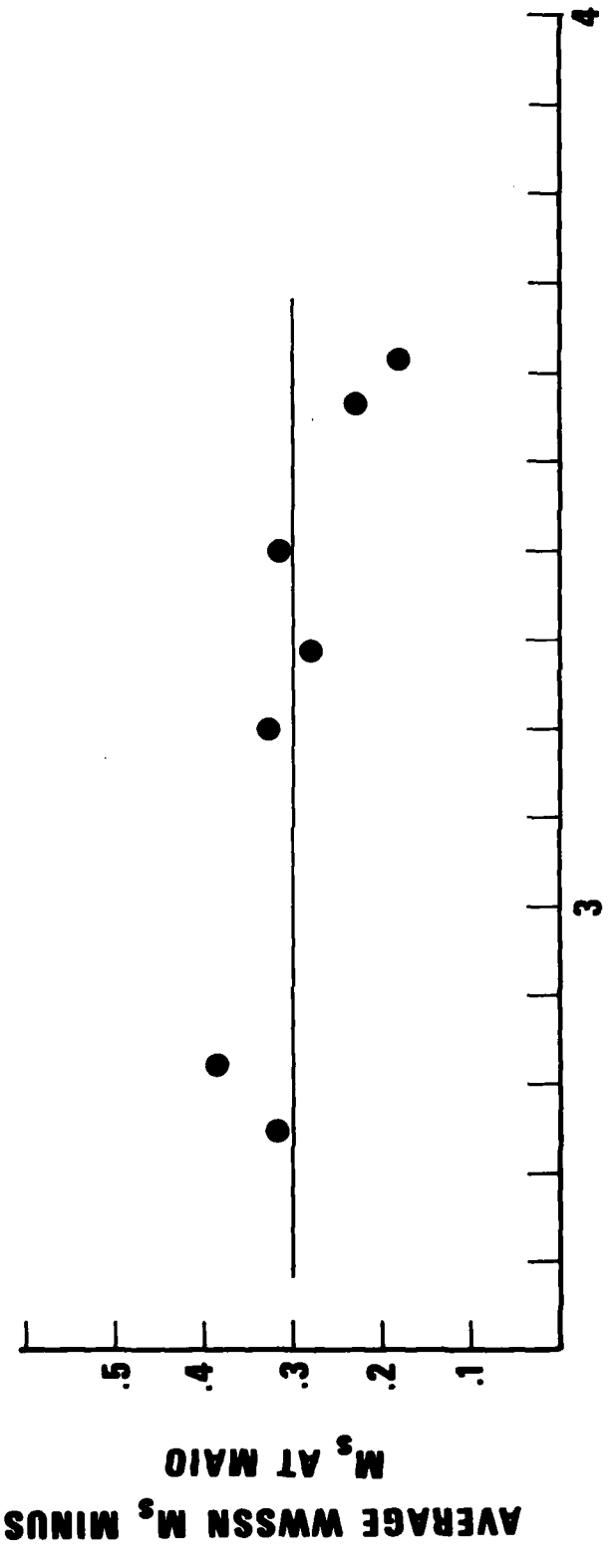

Figure 5. Station bias of 0.3 M_S units is evident when regional M_S values are plotted against WWSSN teleseismic values.

MEASUREMENT OF m_b MAGNITUDES

Summary

In this section it is suggested that the anelastic absorption of P-wave on Gazli-MAIO path ($\Delta = 5.2°$) is less than that on teleseismic paths over which m_b's are generally measured, and that the value of t^* describing the absorption on Gazli-MAIO path is ~ 0.11; that this small absorption causes the m_b measurements of the smaller Gazli shocks made at MAIO to have a positive bias relative to teleseismic measurements, and that this bias can be approximately removed by including an attenuation correction to the m_b determination formula.

Since the agencies NEIS or ISC have given m_b magnitudes only for a few of the larger Gazli aftershocks, we determined m_b's from the MAIO records. We measured amplitudes and periods of P-waves. The periods are plotted against trace amplitude in Figure 6. Periods of the smallest shocks are shorter than periods generally observed at teleseismic distances. For amplitudes less than 50 nm the period is a constant 0.4 ± 0.1 seconds. For larger shocks the period increases with amplitude. The impulse response of the SRO-SP channel has a period of 0.3 seconds. We interpret the constancy of the period at small amplitudes to mean that the SRO system sees the incoming P wave essentially as an impulse with a duration so short that it does not influence the system response waveform. In other words, the P-wave corner frequency has moved above the system pass-band.

We used a set of simulated seismograms to model the amplitude versus period behavior, using a unidirectional pulse of roughly triangular shape to represent the P-wave passing through a constant Q response (Carpenter, 1966) and the SRO-SP response. The absorption required with an infinitely short impulse to lengthen the observed period to 0.4 seconds was equivalent to $t^* = 0.11$ when t^* is defined as

$$\langle Q \rangle = \frac{T}{t^*}$$

where $\langle Q \rangle$ is the mean quality factor on the ray path and T is travel time.

Carpenter, E. W. (1966). Absorption of elastic waves - an operator for a constant Q mechanism, AWRE Report No. 0-43/66, H. M. Stationery Office, United Kingdom.

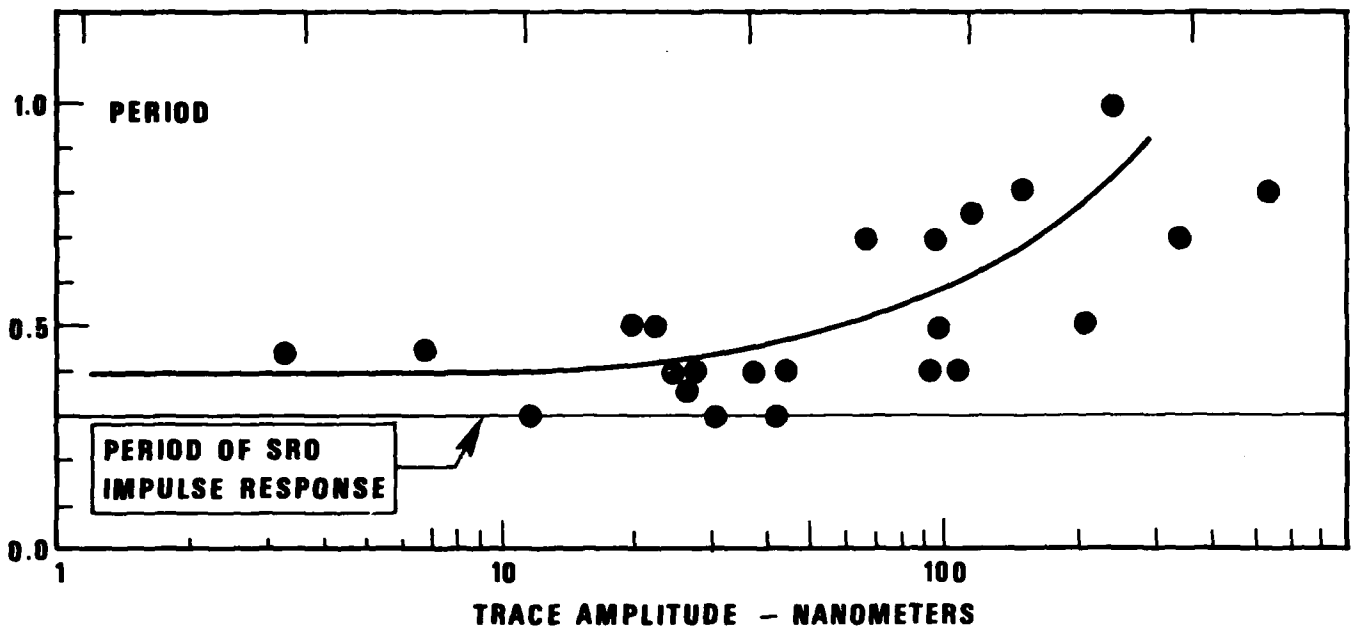

Figure 6. Periods of P_n, Gazli aftershock sequence, plotted against peak-to-peak observed amplitude of P_n. For small shocks the period is constant and equal to about 0.4 sec. As the shock strength increases, the period of P_n gets longer. Thick line gives the simulated period vs. amplitude relationship.

A typical teleseismic value of t* = 0.3 (Der and McElfresh, 1977) would have given a period of 0.54 seconds.

We then assumed the P-wave pulse area I to be proportional to the cube of the pulse width w (half of pulse duration for a triangular pulse) or $I = cw^3$. This proportionality can be derived from the relationship between the seismic moment M_o and the source radius for circular faults with a constant stress drop (Kanamori and Anderson, 1975). Selecting a suitable constant c we can reproduce the amplitude versus period behavior observed in Figure 6, measuring the amplitudes and periods from simulated seismograms using t* = 0.11. The derived relationship is plotted on Figure 6. The value obtained for c was $0 = 38$ nm·s/s^3. Increase of period is caused by increase of pulse duration with amplitude. The set of simulated traces and the input pulses is shown in Figure 7. Note that the waveforms and periods for the three shortest pulses, each with a different duration, is unchanged.

We now simulate seismograms attenuated: (a) by the above determined t* value of 0.11 second and (b) by the assumed teleseismic t* = 0.3 seconds, and compute the difference of the log(A/T) or m_b values between the two sets. The difference is plotted on Figure 8 as a function of amplitude (amplitude when attenuated with t* = 0.11). It is not constant over the range shown, suggesting a positive bias for m_b determinations made at MAIO for small Gazli shocks, even if the distance correction factor in the m_b formula is adjusted to give equal to teleseismic m_b's for the largest shocks in the series.

A simple remedy would be to correct for the larger amplitude along the less attenuating path to MAIO, i.e. for the factor $\exp(0.19\pi/T)$ where 0.19 is the t* difference and T is the period. After this is done, the difference between the simulated MAIO and teleseismic magnitudes becomes nearly constant (and zero) as shown in Figure 8. Also, if the division by T in the m_b formula is neglected at MAIO, the resulting magnitude difference

Kanamori, H. and D. L. Anderson (1975). Theoretical basis of some empirical relations in seismology, Bull. Seism. Soc. Am., 65, 1073-1095.

Der, Z. A., and T. W. McElfresh (1977). The relation between anelastic attenuation and regional amplitude anomalies of short-period P waves in North America, Bull. Seism. Soc. Am., 67, 1303-1317.

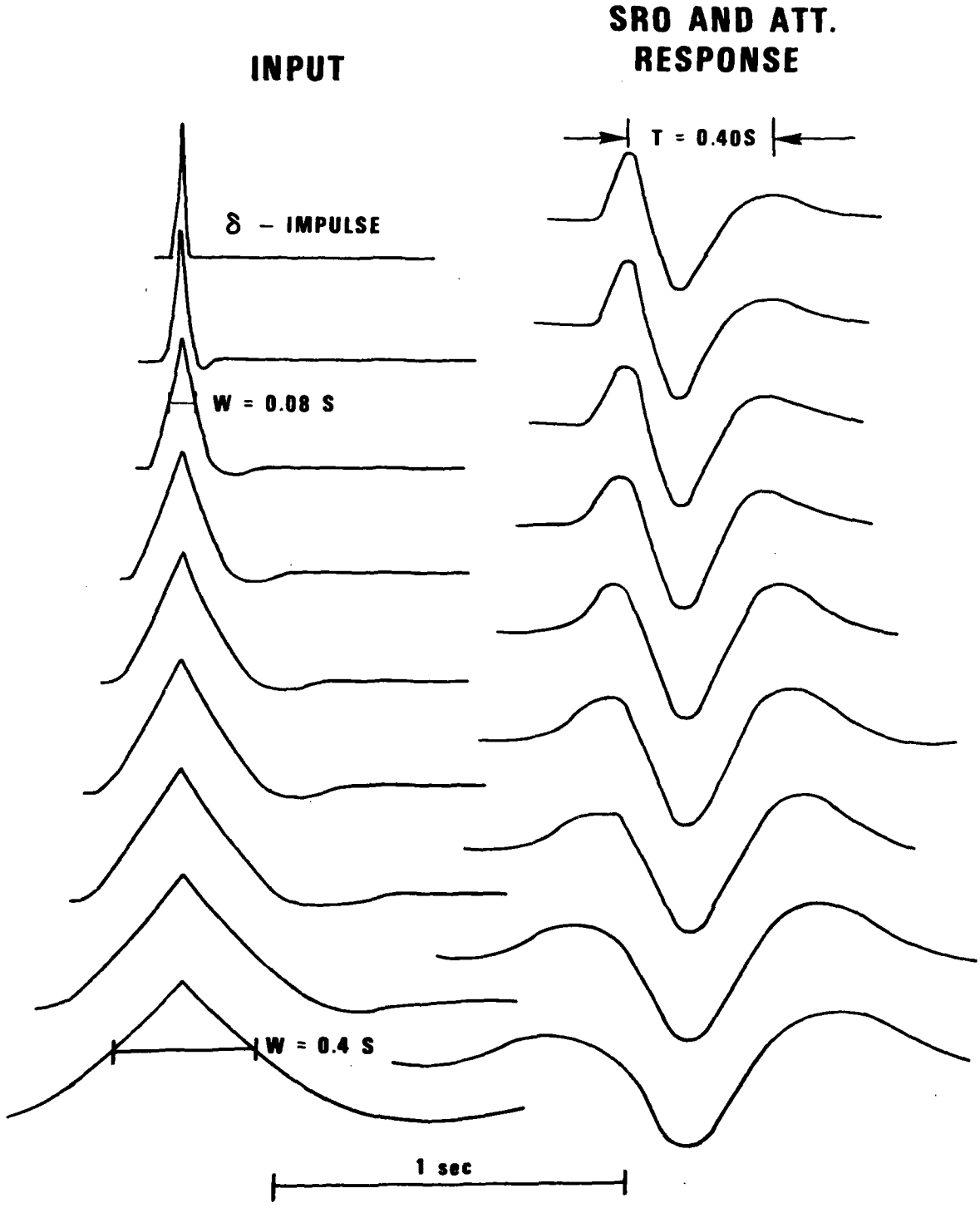

Figure 7. Theoretical response of P-wave signals after modification by attenuation and SRO instrument response.

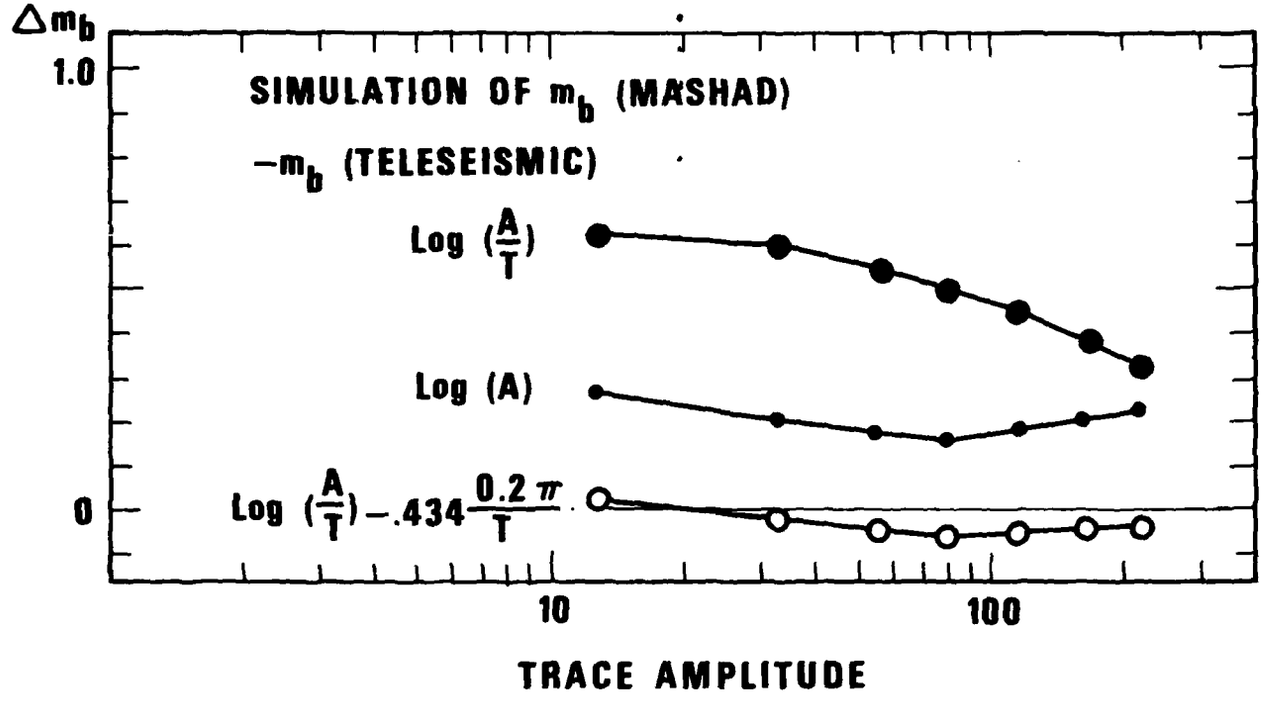

Figure 8. Difference in m_b plotted against Mashad trace amplitude for simulated seismograms using different formulas for Mashad m_b.

is fairly constant, as shown in Figure 8.

We determined the m_b values both by using the attenuation correction and by neglecting the division by T, and then adjusted the respective distance corrections by comparing the m_b values reported by NEIS and ISC for the largest shocks in the series to those computed at MAIO.

The correlation between attenuation-corrected log A/T values and teleseismic m_b's are shown in Figure 9. Adjusting the distance correction for MAIO so that we get, on the average, equal magnitudes, we get the formula for MAIO m_b as

$$m_b = \log \frac{A}{T} - 0.434 \frac{\pi 0.19}{T} + 2.74 \qquad (1)$$

Veith and Clawson's (1972) distance corrections would give

$$m_b = \log \frac{A}{T} + 2.79$$

for crustal shocks at distance 5.2°.

If we use the amplitude only and neglect the division by T, we get, after adjusting the distance correction to agree with NEIS, and ISC m_b's,

$$m_b = \log A + 2.66 \qquad (2)$$

This is close to the value given by Nuttli for Southern Asia (1979) for a distance of 5.2°, or

$$m_b = \log A + 2.57 \qquad (3)$$

Formula (3) was used to determine the m_b values in this study. A is corrected for SRO-SP response at period T in all of the above formulae.

Veith, K. and G. Clawson (1972). Magnitude from short-period P-wave data, Bull. Seism. Soc. Am., 62, 435-452.

Nuttli, O. W. (1979). Personal communication given at the AFOSR Conference, Sheraton International Meeting Center, Reston, Virginia, May 24-25.

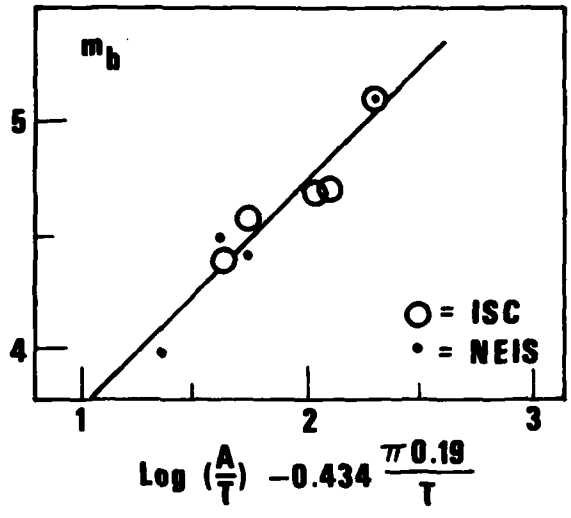

Figure 9. The correlation between attenuation-corrected log A/T values and teleseismic values of m_b.

Additional comments. The $t^* = 0.11$ on the 580 km long P-wave path, of which about 500 km is in the mantle, gives for the mean Q in the top of the mantle a value of 570, if all absorption is assumed to happen in the mantle and none in the crust. If the P-waves recorded at MAIO are head waves, their spectra have the factor $(i\omega)^{-1}$ relative to the free body wave (Grant and West, 1965). Keeping the source waveform an impulse, we get periods larger than 0.4 s in trace simulations of head waves, even with no absorption. The waveform compares poorly with observed P-waves. We suggest that the waves have followed a curved ray path below the Moho discontinuity and are of body wave type. Cerveny and Ravindra (1977) suggest that the diving P wave is more likely to be observed than the head wave at distances larger than a few hundred km in the presence of even a small positive velocity gradient in the top of the mantle.

Cerveny, V. and R. Ravindra (1977). Theory of Seismic Head Waves, Univ. of Toronto Press, Toronto.

Grant, F. S. and G. F. West (1965). Interpretation Theory in Applied Geophysics, McGraw-Hill Book Co., New York.

SIMULATED m_b VERSUS M_s RELATIONSHIP

At amplitudes smaller than 50 nm the P-wave period remains constant (Figure 6) suggesting that the P-wave corner frequency has moved above the system pass-band. We want to test how closely the P-wave amplitude is proportional to the source seismic moment M_o in such a situation under our conditions. A P-wave amplitude proportional to M_o would cause $\partial M_s/\partial m_b = 1$ according to such earthquake dislocation models as advocated e.g. by Savage (1966).

We use the same waveform simulation as in the previous chapter, and plot in Figure 10 the logarithm of area I of the pulse against the m_b computed from the simulated trace. I is proportional to the source seismic moment (Randall, 1971). We use the constant c determined in the previous chapter, $t^* = 0.11$, and compute the m_b in the same way (formula 3) as from real observations.

Assuming I to be proportional to M_o, and log M_o to be equal to $M_s + C$, where C is a constant, Figure 10 suggests $\partial M_s/\partial m_b$ to be = 1 at $m_b < 3.2$, to be close to 2.0 at $m_b > 4.5$, and to be intermediate (~ 1.35) between these values.

Savage, J. C. (1966). Radiation form a realistic model of faulting, Bull. Seism. Soc. Am., 56, 577-592.

Randall, M. J. (1971). Shear invariant and seismic moment for deep-focus earthquakes, J. Geophys. Res., 76, 4991-4992.

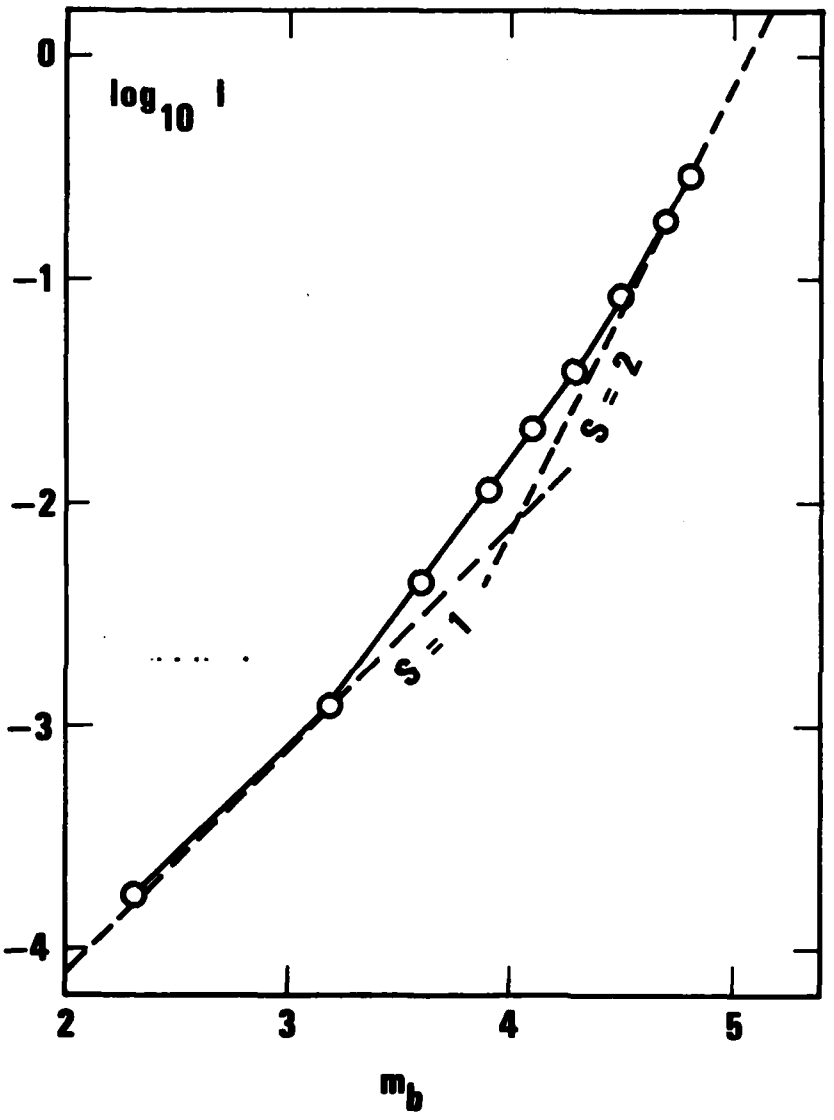

Figure 10. Simulated relation between $\log_{10} I$ (I, the P-wave pulse area, is proportional to seismic moment), and m_b.

OBSERVATIONS OF L_g AND P_n AMPLITUDES

In discrimination seismology, it appears that in many parts of the world, the ratio of maximum L_g amplitudes to P_n amplitudes can be a useful discriminant for signals received at regional distances.

L_g and P_n amplitudes are plotted in Figure 11 for the complete range of event magnitudes that was faithfully recorded by the SRO station at MAIO; that is 3.1 to 5.2 m_b. The values plotted are zero-to-peak amplitudes. The data show that maximum L_g amplitude was between 1.0 and 2.0 times the maximum P_n amplitude, for this particular distance and region.

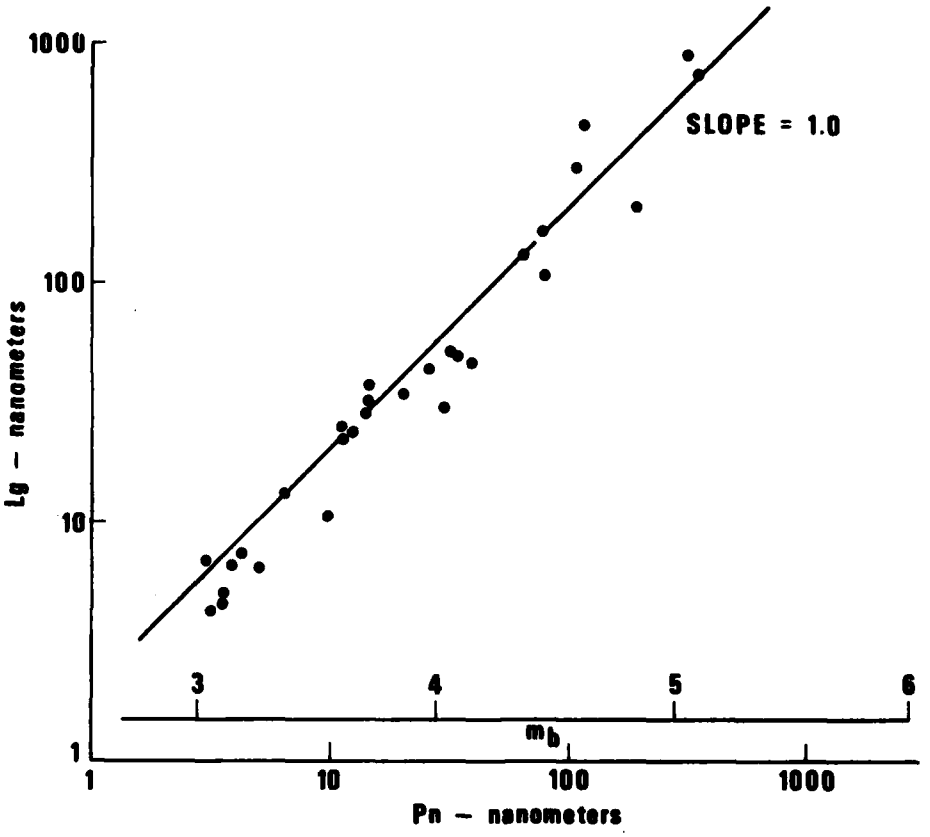

Figure 11. P_n and L_g recorded at MAIO from Gazli earthquake aftershock sequence 8 April 1976.

SATURATION AT SRO STATIONS

If we arrange a set of signals from the Gazli earthquake sequence in order of increasing magnitude, or equivalently, increasing ground motion as experienced at station MAIO, we can see the development of saturation effects in the SRO recording system and how the distortion of the signal shape progresses in both the short-period channel and the long-period channel.

This has been done in Figure 12 where the signals have been aligned so that both short-period and long-period are cotemporal at the arrival of S_n, the largest amplitude phase in the short-period coda. Notice that there is no distortion in either channel until the SP amplitude approaches 1048 nanometers (equivalent ground motion at 1 Hz). This is the clipping level of the SP channel, and the SP signal will never be recorded as a larger digital signal, even if the ground motion is greater. The clipping is visible as a squaring-off of the sinusoidal peaks of the waveform, however.

The situation shows differently on the long-period channel. No digital magnitude limit is obvious; the recorded counts become extremely large instead. The surface wavetrain loses its oscillatory character and tends to become a unipolar pulse with overshoot and exponential damping.

These saturation effects apparently reside in the analogue filter section of the SRO system. The SP channel recovers much more quickly than the LP section, and what one sees is essentially the transient overload response of the LP filter section.

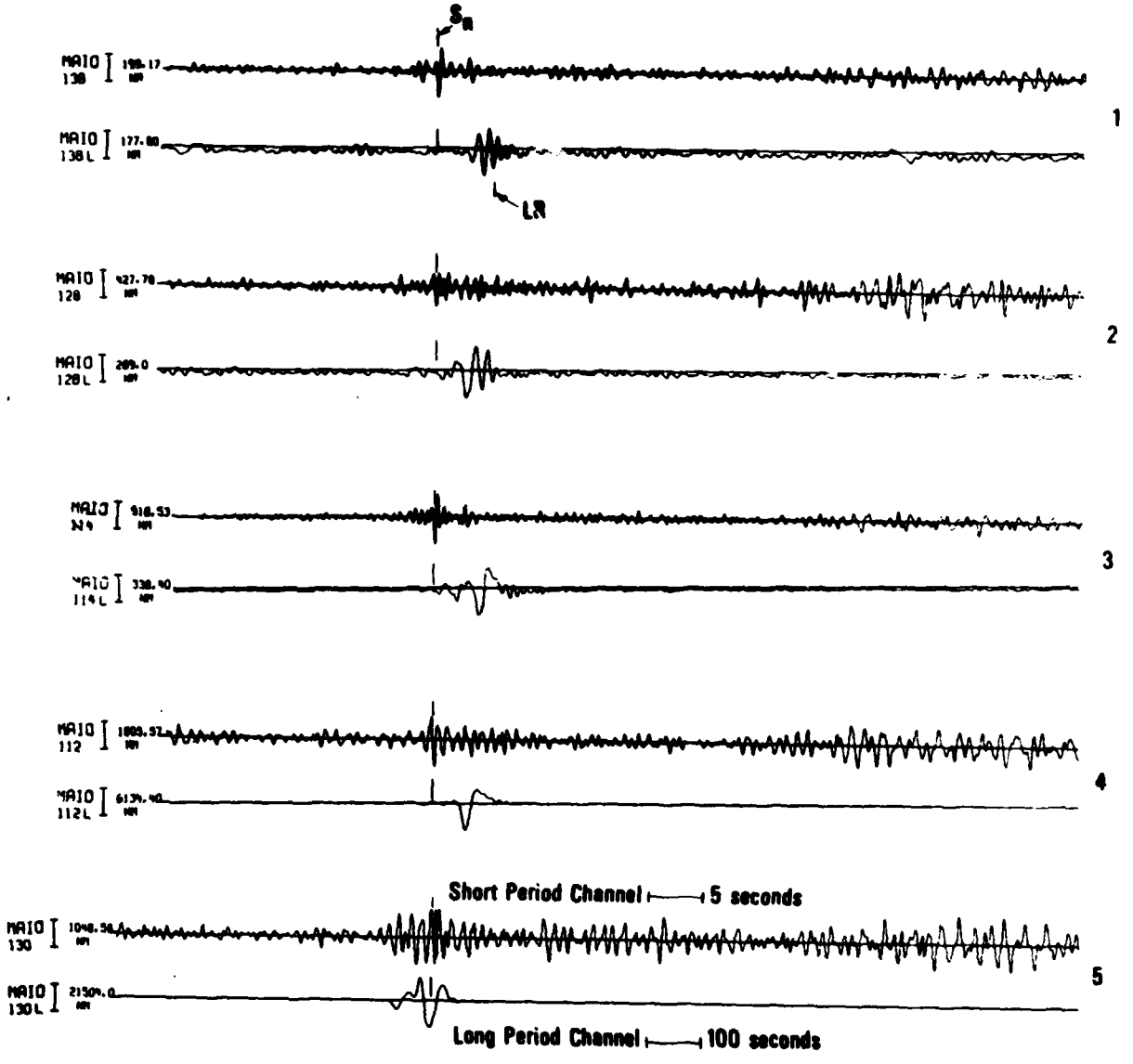

Figure 12. Progressively greater shocks from top trace to bottom, showing development of non-linear recording on the long-period channel. The traces are different sweep speeds, of course, but they are aligned at the instant of time corresponding to the S_n phase.

RESULTS AND CONCLUSIONS

The measurements made as described in the preceding sections are plotted in Figure 13 together with Eurasian measurements made at Norway by Bungum and Tjostheim. The latter consist of earthquakes at distances of 22° to 55° from the receiver, whereas the Gazli sequence is recorded at one fixed distance of 5.2°.

The largest m_b for which an M_s is recordable is $m_b = 5.2$. This limitation is a result of non-linear long-period effects destroying the fidelity of the signal from larger events, even though there were larger events present in the swarm.

The two populations, one teleseismic, and the other regional, are almost overlapping on this M_s:m_b diagram and this implies that there is no large error in our determinations of either M_s or m_b. This is natural since we have calibrated our formulas for measuring M_s and m_b at 5.2° to agree with teleseismic measurements of the same quantities by the WWSSN network and other stations reporting to the ISC.

There is no reason, however, why a systematic difference could not appear between the magnitude determinations in the two populations, since the populations are different. The earthquakes studied by Bungum and Tjostheim are scattered over a region over 60 degrees wide, and thus represent the average M_s/m_b relations measured from a large area and from widely varying fault mechanisms as depths in the crust. Our determinations come from an aftershock sequence in a region less than 1 degree wide, where the shocks also probably tend to have similar fault orientations and depth in the crust. Thus our M_s and m_b values may well reflect regional or source-related anomalies. The absolute position of our population in the m_b versus M_s plot (relative to the other population) may well be uncertain by several tenths of magnitude unit. The two populations should not be combined into one population. Our purpose in trying to estimate reliable absolute M_s and m_b values was to determine how our shocks compare in size with the Bungum-Tjostheim population. As shown in Figure 13, the larger half of our population has sizes comparable with the smallest shocks of the Bungum-Tjostheim population, and the smaller half of our shocks is significantly smaller than any of the Bungum-Tjostheim

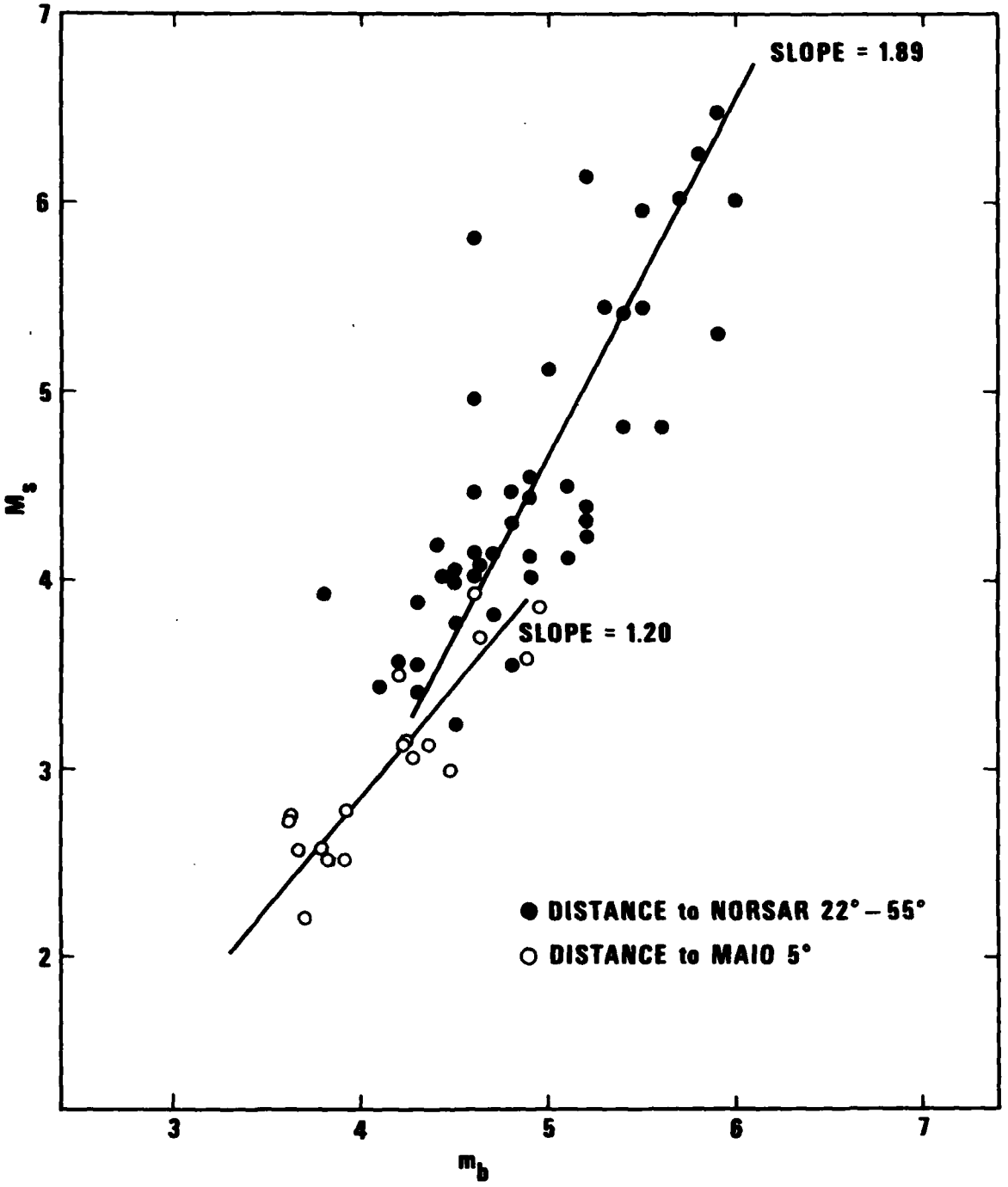

Figure 13. Gazli aftershock sequence (open circles) of events plotted together with Eurasian earthquakes (filled circles) recorded at NORSAR. The straight lines shown are maximum-likelihood slopes assuming equal distributions of error in both M_s and m_b for the two populations separately. The two populations though shown together here, should not be combined into one population because of possible small systematic differences in magnitude determinations.

shocks. Our population thus extends the observations to lower magnitude

The slope of the least-squares line fitted to the Bungum-Tjostheim population is 1.9. The line is fitted assuming the m_b and M_s determinations to have equal and uncorrelated errors (Eriksson, 1971). The slope is close to other M_s versus m_b slope measurements, beginning from the Gutenberg-Richter slope 1.6 (Savino et al., 1971; Marshall and Basham, 1972).

The slope of the line fitted to our population is 1.2 ± 0.3, the latter figure being the standard deviation of the slope. The standard deviation is large because errors are assumed to exist both in m_b and M_s measurements. If we take m_b, or M_s, to be without error we get, respectively, slopes 1.0 ± 0.1, or 1.3 ± 0.1. The main observation is that the slope is significantly smaller than those found for populations of larger shocks.

The prediction that $\frac{\partial M_s}{\partial m_b}$ approaches 1.0, when magnitude decreases below a threshold, is supported by these observations. In Figure 10 we have given a definite form to that prediction.

Tucker and Brune (1977) measured m_b and M_s magnitudes for the aftershock sequence of the San Fernando earthquake of 1971 and found all events to lie within one standard deviation of a line with slope 1 drawn through the data. If we fit a least squares line to their 15 observations covering roughly the same m_b and M_s ranges as our population, we get the slope 1.2 ± 0.2 assuming again m_b and M_s have equal and uncorrelated errors.

Savino, J., L. R. Sykes, R. C. Liebermann and P. Molnar (1971). Excitation of seismic surface waves with periods of 15 to 80 seconds for earthquakes and underground explosions, J. Geophys. Res., 76, 8003-8020.

Eriksson, U. (1971). Maximum likelihood linear fitting when both variables have normal and correlated errors, FOA 4 Report C 4474-A1, Research Inst. of National Defence, Stockholm, 80, Sweden.

Tucker, B. E. and J. N. Brune (1977). Source mechanism and m_b-M_s analysis of aftershocks of the San Fernando earthquake, Geophys. J. R. Astr. Soc., 49, 371-426.

ACKNOWLEDGEMENTS

The idea of using the Gazli aftershock sequence for an $M_s:m_b$ study is due to Dr. R. W. Alewine III. We appreciate Dr. R. R. Blandford's helpful review of this report and suggestions during the project. This work was supported by the Advanced Research Projects Agency and was performed under Contract No. F08606-79-C-0007, monitored by the VELA Seismological Center.

REFERENCES

Bungum, H. and D. Tjostheim (1976), Discrimination between Eurasian earthquakes and underground explosions using the m_b:M_s method and short-period autoregressive parameters; Geophys. J. R. Astr. Soc., 45, 371-392.

Carpenter, E. W. (1966), Absorption of elastic waves - an operator for a constant Q mechanism; AWRE Report No. 0-43/66, H. M. Stationery Office, United Kingdom.

Cerveny, V. and R. Ravindra (1977), Theory of Seismic Head Waves, Univ. of Toronto Press, Toronto.

Der, Z. A., and T. W. McElfresh (1977), The relation between anelastic attenuation and regional amplitude anomalies of short-period P waves in North America; Bull. Seism. Soc. Am., 67, 1303-1317.

Eriksson, U. (1971), Maximum likelihood linear fitting when both variables have normal and correlated errors; FOA 4 Report C 4474-A1, Research Inst. of National Defence, Stockholm, 80, Sweden.

Evernden, J. F. (1971), Variation of Rayleigh-wave amplitude with distance; Bull. Seism. Soc. Am., 61, 231.

Grant, F. S. and G. F. West (1965), Interpretation Theory in Applied Geophysics, McGraw-Hill Book Co., New York.

Kanamori, H. and D. L. Anderson (1975), Theoretical basis of some empirical relations in seismology; Bull. Seism. Soc. Am., 65, 1073-1095.

Marshall, P. D. and D. W. Basham (1972), Discrimination between earthquakes and underground explosions employing an improved M_s scale; Geophys. J. R. Astr. Soc., 28, 431-458.

Nuttli, O. W. (1979), Personal communication given at the AFOSR Conference, Sheratorn International Meeting Center, Reston, Virginia, May 24-25.

Randall, M. J. (1971), Shear invariant and seismic moment for deep-focus earthquakes; J. Geophys. Res., 76, 4991-4992.

Savage, J. C. (1966), Radiation form a realistic model of faulting; Bull. Seism. Soc. Am., 56, 577-592.

Savino, J., L. R. Sykes, R. C. Liebermann and P. Molnar (1971), Excitation of seismic surface waves wtih periods of 15 to 80 seconds for earthquakes and underground explosions; J. Geophys. Res., 76, 8003-8020.

Tucker, B. E. and J. N. Brune (1977), Source mechanism and m_b-M_s analysis of afterhsocks of the San Fernando earthquake; Geophys. J. R. Astr. Soc., 49, 371-426.

Vanek, J., A. Zatopek, V. Karnik, N. V. Konderskaya, Y. V. Rizmichenko, E. F. Savarensky, S. L. Solovev, N. V. Shebalin (1962), Standardization of magnitude scales; Bull. (Isvest.) Acad. Sci. U.S.S.R., Geophys. Ser., 2, 108.

Veith, K. and G. Clawson (1972), Magnitude from short-period P-wave data; Bull. Seism. Soc. Am., 62, 435-452.

von Seggern, David (1977), Amplitude-distance relation for 20-second Rayleigh waves; Bull. Seism. Soc. Am., 67, 405-411.